Dear Editor and Reviewers,

Thank you very much for your letter and for the constructive and insightful comments concerning our manuscript, entitled **"Nascent Eocene Indian Monsoons recorded in oyster shells from the western Indian margin"** (Manuscript ID: **egusphere-2026-1393**).

We sincerely appreciate the time and effort you have dedicated to reviewing our work. Your thoughtful comments and suggestions have been extremely valuable in improving the clarity, scientific rigor, and overall quality of the manuscript. We have carefully considered all comments and have revised the manuscript accordingly.

We have addressed the three main concerns raised by the reviewers in the revised manuscript:

1. Definition of threshold criteria for identifying pristine and potentially diagenetically altered shell zones

We have added a dedicated section to the Methodology that defines the threshold values used to distinguish pristine shell material from zones that may have been affected by diagenetic alteration. This provides a clearer and more objective basis for the screening of the shell material.

2. Absence of a chronological age model and reliance on climate-model-based seasonal assignments

We have incorporated ShellChron-derived ontogenetic age models for both shells. This provides an independent chronological framework for the shell records and allows the seasonal interpretations to be evaluated within a shell-based temporal context, rather than relying on climate-model simulations.

3. Reliance on a single shell and potentially overambitious climatic interpretations

We have revised the analysis to include both pristine shells in the climatic reconstruction. Furthermore, we have substantially refined the interpretations and now base our conclusions primarily on the proxy-derived evidence, with the climate-model simulations used as supporting evidence rather than as the primary basis for interpretation. This has allowed us to moderate the interpretations and ensure that the conclusions remain consistent with the available proxy data.

Based on the interpretations in the revised manuscript, we have modified the title of the manuscript also. In the revised manuscript, the title is: "**Sustained high temperatures and seasonal hydroclimate variability recorded in the middle Eocene oyster shells from the tropical western Indian margin"**

In the detailed response document (attached), we have addressed the reviewers' concerns through additional clarification, revision of the text and figures, and improvements to the presentation and interpretation of our results. We believe that these revisions have substantially strengthened the manuscript.

Please find below our detailed, point-by-point responses to all comments.

For clarity,

Reviewers' comments are presented in blue

Authors' responses are presented in black

Changes made in the revised manuscript are presented in red.

We sincerely thank the Editor and Reviewers again for their constructive feedback and for the opportunity to improve our manuscript. We hope that the revised version satisfactorily addresses all of the concerns raised and will be suitable for publication.

Sincerely,
Aniket Mitra
On behalf of the authors.

REVIEWER 1

Mitra et al studied oyster shells from the Bartonian and compared them to CESM model simulations, concluding that the provenance region experienced weaker monsoonal conditions relative to today. However, there are major flaws in their reasoning and discussions as outlined below.

Firstly, I don't understand why you excluded the other two specimens from your analyses. You state that Fe concentrations are higher in one but the other elements have consistent trends. It is also absolutely not clear and seemingly subjective that the elements associated with dissolution and (re)precipitation (your Na in Figure 4a-b, 4e-f) or structural defects (Si in Figure 4a-c) or diagenesis (Fe in Figure 4a-b, 4d-e) are significantly different between each specimen, leading to the exclusion of two out of three specimens. Also, if the stable isotopes are almost the same for two specimens, why exclude one of them if there is no clear diagenetic signal? Ultimately what your discussion implies is that your entire story is based on only one specimen with four data points, which is not robust for publishing with the conclusions you write. I suggest adding a clear section in the methods on your exact definitions of what you consider to be "well-preserved" or what your preservation criteria are or adjusting your focus to also be that of preservation issues/analyses as well.

Response:

We sincerely thank the reviewer for this important comment and agree that the criteria used to assess shell preservation and the rationale for specimen selection required greater clarity. In the revised manuscript, we have therefore provided a more explicit and quantitative description of the preservation criteria adopted for palaeoclimate reconstruction, based on published studies and the elemental thresholds (Fe and Mn <800 µg/g) discussed in the Materials and Methods **(lines 171-182)**.

We would like to clarify that K/PK/03 was excluded from conventional stable ($\delta^{13}C_{cc}$ and $\delta^{18}O_{cc}$) and clumped isotope (Δ_{47}) analyses, whereas both K/PK/01 and K/PK/02 were retained for conventional stable-isotope analyses. The exclusion of K/PK/03 was based on its consistently elevated Fe concentrations in both analysed transects, together with extensive portions of the section showing low Ca (<38 wt%) and elevated Si (>0.3 wt%). These characteristics indicate a substantially higher likelihood of alteration and/or secondary mineral incorporation compared with the other two specimens **(Lines 314-321)**.

The selection of K/PK/02 for clumped isotope analysis was based on the following reasons:

1. **Elemental preservation:** K/PK/02 consistently exhibits Fe concentrations below 300 µg/g throughout the analysed section, indicating comparatively better preservation. In contrast, K/PK/01 contains three distinct intervals with Fe concentrations exceeding our preservation threshold. Notably, the interval at approximately 2 mm along the growth direction of K/PK/01 is also associated with markedly lower $\delta^{18}O_{cc}$ value, further raising concerns regarding its suitability for high-precision clumped isotope thermometry **(314-318)**.

2. **Elemental/Ca behaviour:** K/PK/01 exhibits a progressive change in baseline elemental/Ca values along the growth direction, particularly in Na/Ca, Mg/Ca, and Cu/Ca, and to a lesser extent in Sr/Ca and Ba/Ca. In contrast, K/PK/02 displays predominantly quasi-cyclic variations without a comparable progressive baseline shift. Because elemental concentrations and stable-isotope compositions may reflect a combination of environmental conditions, climate variability, and biological/vital effects, we considered K/PK/02 to provide the more internally consistent record for clumped isotope thermometry and thereby minimised the potential influence of these confounding factors **(Lines 538-541)**.

Importantly, the exclusion of K/PK/01 from clumped isotope analysis does not imply that the specimen was considered unsuitable for the study. Both K/PK/01 and K/PK/02 were retained for conventional stable-isotope analyses. The four clumped isotope temperature estimates based on 9-11 replicates of each sample from K/PK/02 were used primarily as independent temperature constraints rather than as a standalone reconstruction of seasonal temperature variability. These temperature estimates show correspondence with the independently developed ShellChron growth model (de Winter, 2022) and the assigned seasonal positions in both K/PK/01 and K/PK/02, based on the month estimates from ShellChron growth model. In addition, the temperature-$\delta^{18}O_w$ relationship was evaluated using 19 paired observations derived from the two specimens (10 from K/PK/01 and 9 from K/PK/02). Thus, the interpretation is not based solely on four clumped isotope analysed derived temperature estimates, but on the integration of clumped isotope temperatures with conventional oxygen and carbon isotopes, elements/Ca profiles, the ontogenetic age model, and climate-model simulations **(Lines 505-511, 528-532)**.

We fully agree with you that a larger number of specimens with clumped isotope analyses would provide stronger statistical constraints. However, *Pycnodonte kachchhensis* shells preserved in-situ within the Fulra Limestone are exceptionally scarce, and only three specimens suitable for palaeoclimatic investigation could be recovered. We have therefore explicitly acknowledged this limitation in the manuscript and have been careful not to overstate the strength of the reconstruction.

We have also substantially revised the interpretation presented in the primary submission of the manuscript. In particular, we have removed the previously proposed interpretation of a probable monsoon signal, which was not sufficiently constrained by the available data. Instead, the revised interpretation is more conservative and focuses on the identification of reoccurring seasonal intervals characterised by conditions in which precipitation exceeded evaporation or vice versa along with the temperature signals. These interpretations are based on the integrated evidence from the stable-isotope records of both shells, the four clumped isotope temperature estimates (9-11 replicates each), trace element/Ca profiles, the independently constrained growth chronology, and climate-model simulations. Accordingly, we now interpret the record as evidence for seasonal hydroclimatic variability, although representing a minimum seasonal estimate, rather than assigning these variations specifically to nascent monsoon signal **(Lines 693-702)**.

Lines 171-182:

3.5 Preservation of shells and analysis strategy

Analysis of well-preserved shell carbonate is essential for conventional isotope and clumped isotope thermometry based palaeoseasonality studies, as recrystallisation of biogenic calcite can reset the Δ_{47} signal and yield temperatures representative of diagenetic alteration rather than primary shell formation (Douglas et al., 2014; de Winter et al., 2018; Davies et al., 2023). Mn and Fe enrichment is widely associated with diagenetic alteration of biogenic calcite (Al-Aasm and Veizer, 1986; Steuber, 1999). Following the Cretaceous *Pycnodonte vesicularis* preservation assessment of de Winter et al. (2018), in which Mn or Fe concentrations >800 µg/g were identified as indicative of recrystallised shell carbonate, we adopted 800 µg/g as a conservative screening threshold for subsequent stable isotope analyses. Clumped isotope analyses were restricted to the shell(s) with Fe and Mn concentrations below the predefined thresholds throughout the analysed region to establish an independent temperature framework for interpreting the subsequent stable-isotope record and reconstructing seasonal variability.

Lines 316-323:

In contrast, K/PK/03 shows consistently higher Mn and Fe concentrations, averaging 192 μg/g and 725 μg/g, respectively, particularly near the ventral end of the resilifer where Ca falls below 38.0 wt% and Si exceeds 0.3 wt% (Fig. 3c). Elevated concentrations of Mn and Fe are observed in areas with high Si and low Ca levels (Fig. 3). Three discrete, thin bands with Fe concentrations exceeding the threshold are identified along the resilifer-edge transects of K/PK/01, whereas K/PK/03 is characterised by Fe concentrations consistently above the threshold. In contrast, K/PK/02 remains below the Fe and Mn thresholds throughout the analysed profile. Away from the resilifer edge, however, all analysed sections exhibit elevated Fe concentrations above the threshold (Fig. 3).

Lines 538-541:

Large-ion lithophile elements (LILEs; Sr and Ba) and REEs (eg. La) exhibit clear quasi-cyclic variability in the well-preserved shells (K/PK/01, K/PK/02), whereas the systematic trends in Na, Mg, and Cl in K/PK/01 suggest evolution of baseline value (Fig. 7). This type of baseline value evolution is also seen in Cretaceous Pycnodonts (de Winter et al., 2018). Although Sr and Ba show minor effect of baseline fall in K/PK/01, their quasi-cyclic variability remains well preserved.

Lines 510-518:

Both of the $\delta^{18}O_{cc}$ and LILE/Ca profiles in K/PK/01 and K/PK/02 exhibit three annual cycles, and the ShellChron age model independently yields ~36 months of recorded ontogenetic growth, with no evidence of repetitive seasonal growth cessation (Fig. 4). The estimated highest SST (D_{47}-T: $35.8^{+2.8}_{-2.7}$ °C; $\delta^{18}O_w$: $1.2^{+0.5}_{-0.5}$ ‰) point of month seven of K/PK/02 is aligned with May, the warmest month of a year, according to the modern Indian climatic scenario and CESM simulations of the Eocene (Fig. 7). Accordingly, the rest of the three clumped isotope temperature estimates from multiple replicates (9, 9 and 11 respectively) correspond to January-February (D_{47}-T: $31.3^{+2.2}_{-2.1}$°C; $\delta^{18}O_w$: $0.6^{+0.4}_{-0.4}$ ‰), June-July (D_{47}-T: $33.5^{+3.7}_{-3.6}$ °C; $\delta^{18}O_w$: $0.8^{+0.7}_{-0.7}$ ‰) and April-May (D_{47}-T: $35.6^{+3.0}_{-2.9}$ °C; $\delta^{18}O_w$: $1.6^{+0.6}_{-0.5}$ ‰). The observed range of temperature variation should be carefully interpreted as minimum seasonality estimates, due to the low sampling resolution required to obtain enough material for robust clumped isotope analysis.

Lines 528-532:

The January-February, April-May, and June-July intervals identified in the K/PK/01 and K/PK/02 shell chronologies were assigned temperatures from the independent clumped isotope averages of those months based on 9-11 replicates each. Corresponding $\delta^{18}O_w$ values from those points (10 points of K/PK/01 and 5 points of K/PK/02) were calculated using the Kim and O'Neil (1997) equation ($\delta^{18}O_{w\ VSMOW}$ =[(1000+$\delta^{18}O_{cc}$)/exp{18.03/(D_{47}-T+273.15)- (32.42/1000)}]-1000) from the SST estimates (°C) and respective $\delta^{18}O_{cc}$ values (in VSMOW) along the shell transects.

Lines 693-702:

Proxy-based reconstruction from the multi-year archive of the pycnodont shells, supported by climate model simulations, reveal small seasonal temperature difference (DSST: ~5 °C: 31-36 °C) comparable to modern north India (DSST: ~7 °C: 23-30 °C). The region likely maintained generally more extreme sea-surface temperatures than the present Gulf of Kutch, with rainfall-driven cooling events associated with typical reduced evaporation for at least twice a year with a gap of ~7-8 months. Rainfall occurring ~8-9 months after peak summer had been facilitated by the advection of moisture from the open Tethys Seaway between India and Eurasia. Although the limited sampling points with large material requirements for robust D_{47}-temperature estimates do not permit reconstruction of the complete seasonal and the monsoon structure, but represent minimum seasonality. However, the identification of lower $\delta^{18}O_w$ during ~1-2 and ~8-9 months after peak summer provides evidence for a seasonally structured hydrological cycle in the late Bartonian India, different in character from modern four month confined summer monsoon of north India.

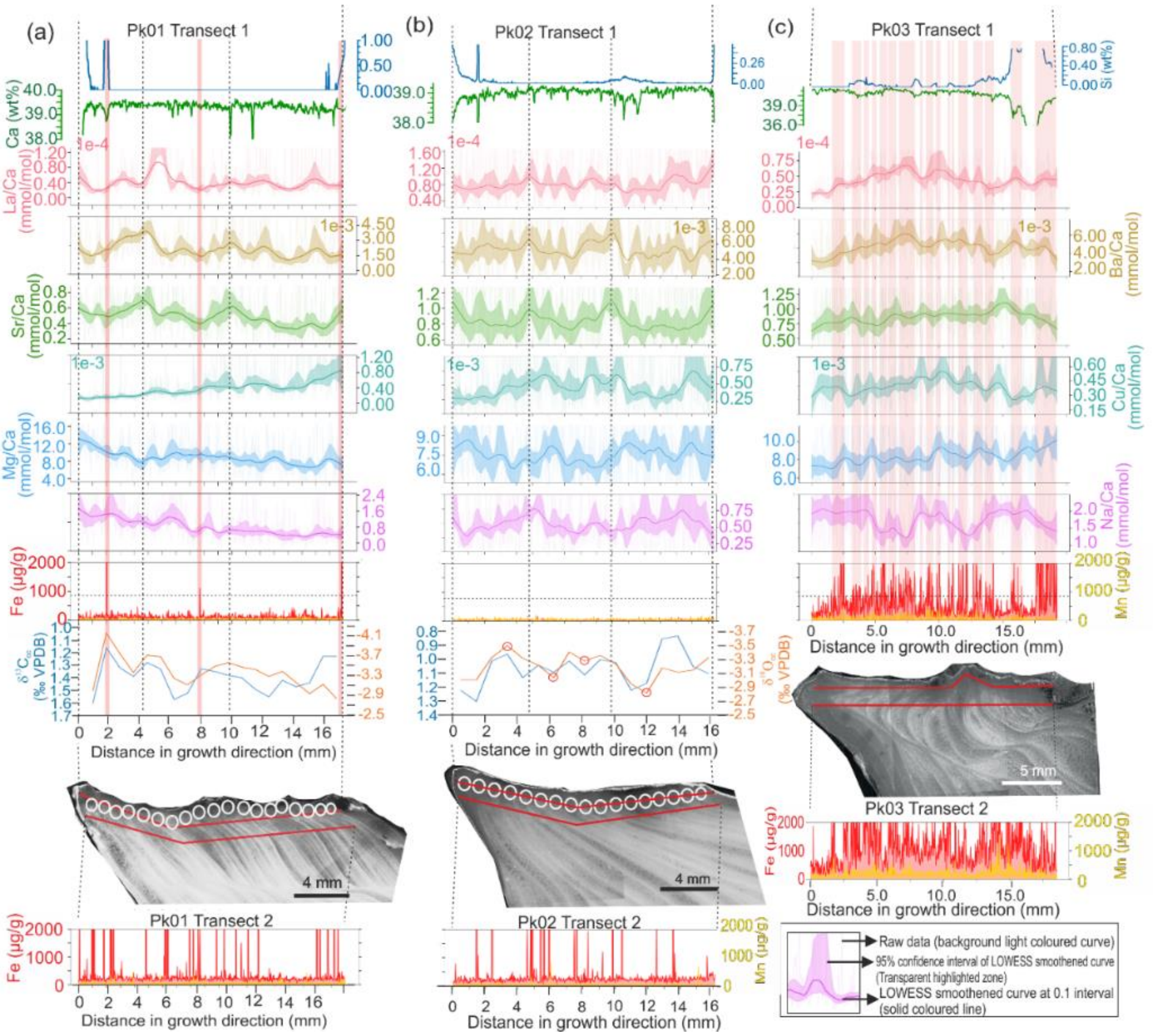

Figure 3. Plots of Ca and Si wt%, manganese (Mn) and iron (Fe) concentrations along with trace element-to-calcium ratios, measured along the growth axes of the resilifers in *P. kachchhensis* shells from resilifer edge transects of (a) K/PK/01 (b) K/PK/02 and (c) K/PK/03; and Mn, Fe concentrations from transects 2mm away from the resilifer edges at the bottom of the respective specimens. Red circles on $\delta^{18}O_{cc}$ profile of K/PK/02 indicate clumped isotope analyses points. Dotted vertical lines are indicative of probable year-markers. The line scan profiles are plotted on the cross-section image by red lines; white circles indicate stable isotope sampling points. Representative trace element-to-calcium ratio profiles from each element category (light metal, large ion lithophile elements, transition metals and rare earth elements) are shown. All trace element-to-calcium profiles is shown in supplementary file Fig. S4.

Secondly, the lack of a clear definition of what you define as seasons or the lack of a clear growth curve leaves the reader confused as to how robust your conclusions actually are. What if growth stop(s) occurred and you interpret your $\delta^{18}O$ to be a different month than it is, such as your second datapoint being the winter and third your second year summer or the whole specimen being one year, your whole story would change and no concrete conclusions could be made on the monsoon in the Bartonian. Your element ratio profiles have three to four peaks, suggesting more seasons/years than you currently consider for example.

Response:

We sincerely thank you for this important suggestion. In the revised manuscript, we have incorporated an explicit shell-growth chronology for both K/PK/01 and K/PK/02. The chronology is developed using high-resolution Sr/Ca profiles acquired at 25 µm resolution along the growth axes and integrated with the $\delta^{18}O_{cc}$ profiles to identify recurrent seasonal cycles and constrain annual markers. The resulting chronology is generated using ShellChron (de Winter, 2022), followed by a Monte Carlo post-processing approach following Han et al. (2026) to account for uncertainties in the age-distance relationship (**Lines 245-261**).

The resulting growth model provides an internally consistent age-distance framework that allows the positions of the conventional stable and clumped isotope analysis, as well as the trace-element profiles, to be assigned to approximate ontogenetic months (**Lines 357–365**). Importantly, this approach does not assume a constant growth rate throughout the shell; rather, variations in growth rate are shown by the model and discussed as well. This substantially reduces the possibility that a growth slowdown or interruption would be incorrectly interpreted.

We have also revised our interpretation of the number of annual cycles in response to your and Reviewer 2 observation regarding the multiple peaks in the elements/Ca profiles. The combined $\delta^{18}O_{cc}$ and quasi-cyclic trace element records indicate at least three recurrent annual cycles, which are now incorporated into the revised chronology. We therefore do not interpret the individual isotope variations solely on the basis of their position along the shell, but within the independently constrained growth framework.

We believe that this revised approach provides a substantially more robust basis for evaluating seasonal variability and avoids the ambiguity associated with assigning individual isotope measurements to particular months solely from their spatial position along the shell.

Lines 245-261:

3.9.2 Shell chronology

Shell chronology was estimated based on $\delta^{18}O_{cc}$ and trace element profiles along the growth axis of the resilifer of the shells, K/PK/01 and K/PK/02. K/PK/03 is excluded from the chronologic study, since we consider it diagenetically altered. We used the close correspondence between quasi-cyclic nature of large-ion lithophile elements (LILE: Sr, Ba) and REEs (La, Ce, Pr, Nd, Sm)/Ca (see Sections 4.3, 5.4) and $\delta^{18}O_{cc}$ variability as an indication that Sr/Ca captures seasonal variability in the pycnodont shells (as noted in de Winter et al., 2018). While the exact relationship between Sr/Ca ratios in molluscs and seasonal growth and temperature variability is poorly constrained (see e.g. Lorrain et al., 2005; Freitas et al., 2006), we interpret periodic variations in Sr/Ca coinciding with those in $\delta^{18}O_{cc}$ as the best approximation for seasonal growth. Probable age markers along the oyster growth axes were identified using the well-established seasonal $\delta^{18}O_{cc}$ signal in conjunction with Sr/Ca cyclicity, where peaks of Sr/Ca come after the minimum values of $\delta^{18}O_{cc}$. A continuous, high-resolution (25 µm) Sr/Ca profile was incorporated into the ShellChron growth model (de Winter, 2022) to transform the trace-element records from distance to a seasonally constrained chronological domain. Because ShellChron can produce age inversions in high-resolution datasets, whereby a subsequent data point is assigned a younger age than its predecessor, the resulting age models were subsequently post-processed using a Monte Carlo approach following Han et al. (2026). This approach simulates shell growth through ontogeny while accounting for the uncertainty in the ShellChron output, thereby eliminating age inversions and generating a more realistic and continuous age model for complex datasets while remaining true to the seasonal growth rate distributions estimated by ShellChron.

Lines 357-365:

The monthly resolved chronologies generated by ShellChron for the two best-preserved *Pycnodonte* shells, K/PK/01 and KPK/02 record approximately 36 months of ontogenetic growth (Figs. 4, S5). Resilifer accretion was broadly uniform, with ~5-7 mm of resilifer growth per year, corresponding to an estimated shell-length increment of ~44-64 mm/year (K/PK/01: analysed resilifer 16 mm, shell height 142 mm; K/PK/02: analysed resilifer 17 mm, shell height 156 mm). Distinct periods of reduced growth occur at months 0-6, 22-27, and 33-36 in K/PK/01, and 0-2, 9-15, and 25-28 in K/PK/02 (Fig. 4). As growth rate is not uniform, the 1-mm-spaced stable-isotope measurements results in uneven age spacing with an average of 5-7 measurements per year with a ~2 months resolution of analysis. The four robust clumped isotope temperature estimates, based on 9-11 replicates each correspond to months ~7, 16, 21 and 30 respectively according to the ontogenic age of the specimen K/PK/02 based on the growth rate model.

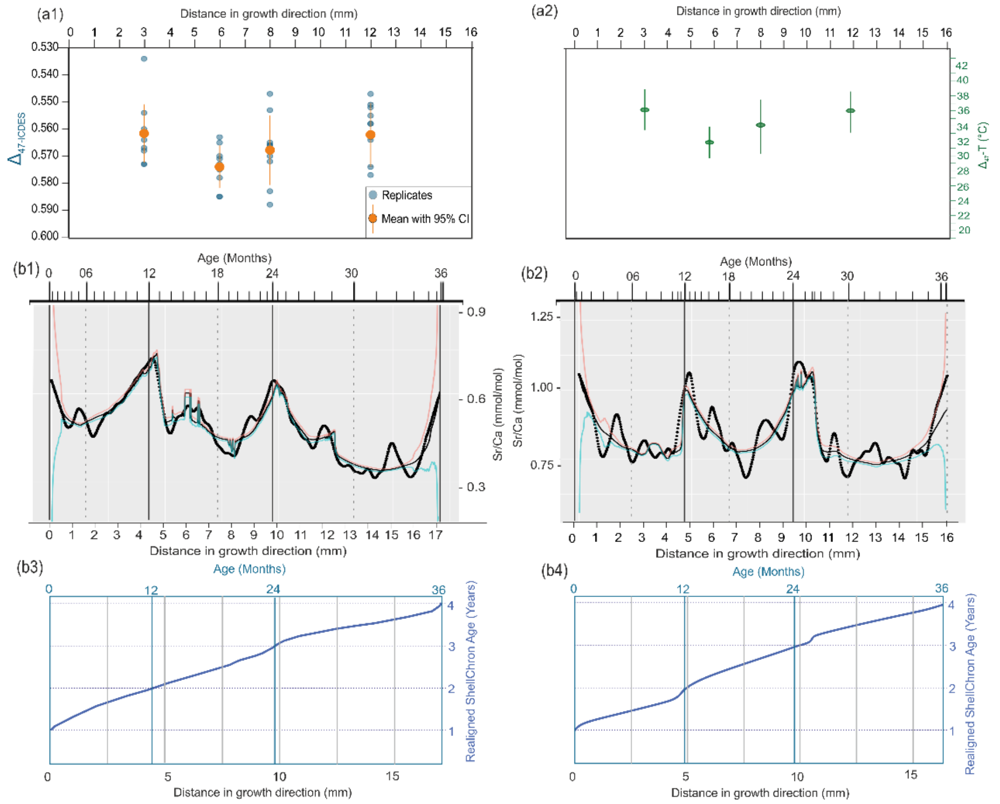

Figure 4. (a) Clumped ($\Delta_{47\ \text{I-CDES}}$) isotope results: (a1) Average values along with 95% CI and all the replicates from the respective points are plotted alongside the distance of shell resilifer growth profile of K/PK/02, (a2) estimated temperatures (Δ_{47}-T) are plotted along the growth profile of K/PK/02; (b) Chronologic shell growth of (b1) K/PK/01 and (b2) K/PK/02, as modelled by ShellChron (de Winter, 2022) based on the high resolution (25 µm) Sr/Ca profile recorded from the resilifer

regions of the shells. Resulting age models were post-processed using a Monte Carlo approach for (b3) K/PK/01 and (b4) K/PK/02 following Han et al. (2026).

Thirdly, your entire conclusion and proxy-model comparison is based on four clumped isotope datapoints from one specimen. Even though it does take time and lots of material to measure clumped isotopes in carbonates, most studies still report at least more than the small handful of datapoints and come to less conclusions than this study does. While the temperature and inferred hydrology signal from clumped isotopes are the main focus of this study, there is much more data from the elemental ratios and on more specimens but almost no discussion of this. You need to either shift the focus to discuss these ratios more or make less grand conclusions from your limited dataset.

Response:

We have revised the manuscript to make clear that the interpretation is not based on the four clumped isotope temperature estimates (based on 9-11 replicates each) alone, but on the integration of clumped isotope temperatures, conventional stable isotopes, trace-element/Ca profiles, and the independently constrained shell-growth chronology from both K/PK/01 and K/PK/02.

The four clumped isotope temperature estimates from K/PK/02 are used primarily as independent temperature reference points that anchor specific positions within the ShellChron-derived monthly chronology. The temperature-$\delta^{18}O_{cc}$ relationship established from these measurements is then used to estimate $\delta^{18}O_{w}$ at the corresponding positions. Combined with the conventional stable-isotope profiles from both specimens and their multiannual (~3 year) growth chronologies, this provides 19 month-specific temperature-$\delta^{18}O_{w}$ estimates (10 from K/PK/01 and 9 from K/PK/02). Thus, the 19 points are regarded as an integrated proxy reconstruction constrained by the four clumped isotope (with 9-11 replicates each) estimated temperature anchors **(see Lines 510-518, 528-532 in response to first feedback)**.

We have also strengthened the treatment of the element/Ca records in the revised manuscript. The quasi-cyclic variations in the trace-element profiles, particularly the large-ion lithophile elements (Sr/Ca and /BaCa) ratios, are now discussed alongside the stable-isotope records and shell-growth chronology **(Lines 547-584, 598-601)**. These profiles provide an independent record of recurrent environmental variability and, importantly, help constrain the identification of repeated annual cycles in the shells. Consequently, the revised interpretation gives greater weight to the multi-proxy evidence from both specimens, rather than treating the clumped isotope data as the sole basis for the palaeoclimate reconstruction.

In accordance with your suggestion, we have also substantially tuned down our conclusions. In particular, we have removed the stronger interpretation of a probable monsoon signal presented in the original manuscript **(see Lines 693-702 in response to first feedback)**. The revised manuscript does not attempt to reconstruct a monsoon history from the four clumped isotope temperature estimates. Instead, we focus on the evidence for persistent high temperatures, relatively low seasonal temperature amplitude, and recurring seasonal hydroclimatic variability, as supported by the integrated conventional stable isotope, clumped isotope, elemental/Ca, and growth chronology records.

Lines 547-584:

Large-ion lithophile elements (LILEs; Sr and Ba) and REEs (eg. La) exhibit clear quasi-cyclic variability in the well-preserved shells (K/PK/01, K/PK/02), whereas the systematic trends in Na, Mg, and Cl in K/PK/01 suggest evolution of baseline value (Fig. 7). This type of baseline value evolution is also seen in Cretaceous Pycnodonts (de Winter et al., 2018). Although Sr and Ba show minor effect of baseline fall in K/PK/01, their quasi-cyclic variability remains well preserved. Therefore, Sr/Ca was selected for age modelling as it provides a robust seasonal signal in *Pycnodonte* (de Winter et al., 2018). The variation of LILEs corresponds with the SST, $\delta^{18}O_w$ and $\delta^{18}O_{cc}$ variation pattern, where Sr/Ca maxima occurring slightly after the temperature and $\delta^{18}O_w$ maxima and $\delta^{18}O_{cc}$ minima (Fig. 7). Regardless of the exact month assignment, the alignment of the ontogenetic age model with trace-element profiles demonstrates strong seasonal control in LILE and REE incorporation for pycnodonts in the equatorial lagoonal setting of the Eocene.

Sr/Ca, Ba/Ca, La/Ca show seasonal variation with peaks corresponding to September-October. CESM simulations indicate that India experiences peak precipitation during these two months (Fig. 8; Baatsen et al., 2020). Although proxy based temperature- $\delta^{18}O_w$ values are unavailable for these intervals (September-October), the observed decline in reconstructed temperature and consistent $\delta^{18}O_w$ decrease from April to July with the model-simulated increase in precipitation (Fig. 8), providing independent support for the inferred seasonal hydroclimatic pattern. Sr incorporation in calcitic shells has been shown to increase with higher precipitation rates in inorganic calcite (Morse and Bender, 1990). Additionally, Eocene bivalves from North Sea records higher Sr and Ba during months of freshwater influx, as terrestrial run-offs contain much higher rate of these elements (Kniest et al., 2024). Increased Ba/Ca ratio is commonly associated with blooms of specific phytoplankton species (Goodwin et al., 2013; Poitevin et al., 2020; Fröhlich et al., 2022). The strong covariation between $\delta^{13}C_{cc}$ and Ba/Ca, with coincident maxima during inferred high-rainfall intervals, is consistent with enhanced primary productivity associated with seasonal terrestrial nutrient delivery associated with fresh-water influx (Goodwin et al., 2013). Similar rainfall-associated productivity increases have been documented in tropical and equatorial coastal lagoons (Herrera-Silveira, 1998; Soondur et al., 2021; Cutrim et al., 2026), supporting a potential link between seasonal runoff and phytoplankton productivity in the Eocene equatorial Kutch setting. Seasonal influences are evident, with peak concentrations of a few trace elements typically observed during the months of increased phytoplankton productivity and/or enhanced fluvial input enriched in trace metals (Liu et al., 2021). While REE incorporation is generally minimally affected by seasonality within a 5-20 °C range (Mouchi et al., 2020), the significantly higher temperatures (30-36 °C) during the late Bartonian India likely influenced REE uptake.

Because Na/Ca, Mg/Ca, and Cu/Ca in the K/PK/01 specimen show strong ontogenetic trends that may obscure seasonal variability, their incorporation mechanisms are beyond the scope of this study, as their clear variation is seen in only one specimen, K/PK/02. However, their quasi-cyclic patterns in K/PK/02 suggest a potential seasonal component, which we briefly interpret in light of published literatures. Mg/Ca profiles, commonly interpreted as a palaeotemperature proxy in oyster shells (Surge and Lohmann, 2008; Bougeois et al., 2014; Durham et al., 2017), shows multiple peaks within a year and does not strongly covary in the pycnodonts with seasonal temperature and/or hydroclimate dynamics based on our conventional stable and clumped isotope analyses (Fig. 7). Its antiphase relationship with the Sr/Ca shows a pattern but failing to strictly follow the temperature dynamics and respective months proves that it is affected by salinity, water Mg/Ca ratio, growth, metabolism, and ontogeny (Putten et al., 2000; Schöne et al., 2010; Freitas et al., 2009; Mouchi et al., 2013). This highlights Mg/Ca profiles limitations in restricted, evaporative or freshwater-influenced environments (Tynan et al., 2017). The Na/Ca ratio in bivalve shells has been used as a palaeosalinity proxy (Golan et al., 2016; Higuera-Ruiz and Elorza, 2009), although its environmental signal can be substantially modulated by growth dynamics (Marali et al., 2017; Arndt et al., 2023), consistent with the latter mechanism observed in our record of K/PK/01. Transition metals such as Cu are incorporated into shells from suspended and dissolved phases, modulated by physiology and environment (Huanxin et al., 2000). Because Cu uptake into oyster shells is generally favoured in lower salinity conditions (Huanxin et al., 2000), we interpret elevated Cu/Ca ratios to elevated palaeo-rainfall for monsoon and post-monsoon months (Fig. 7).

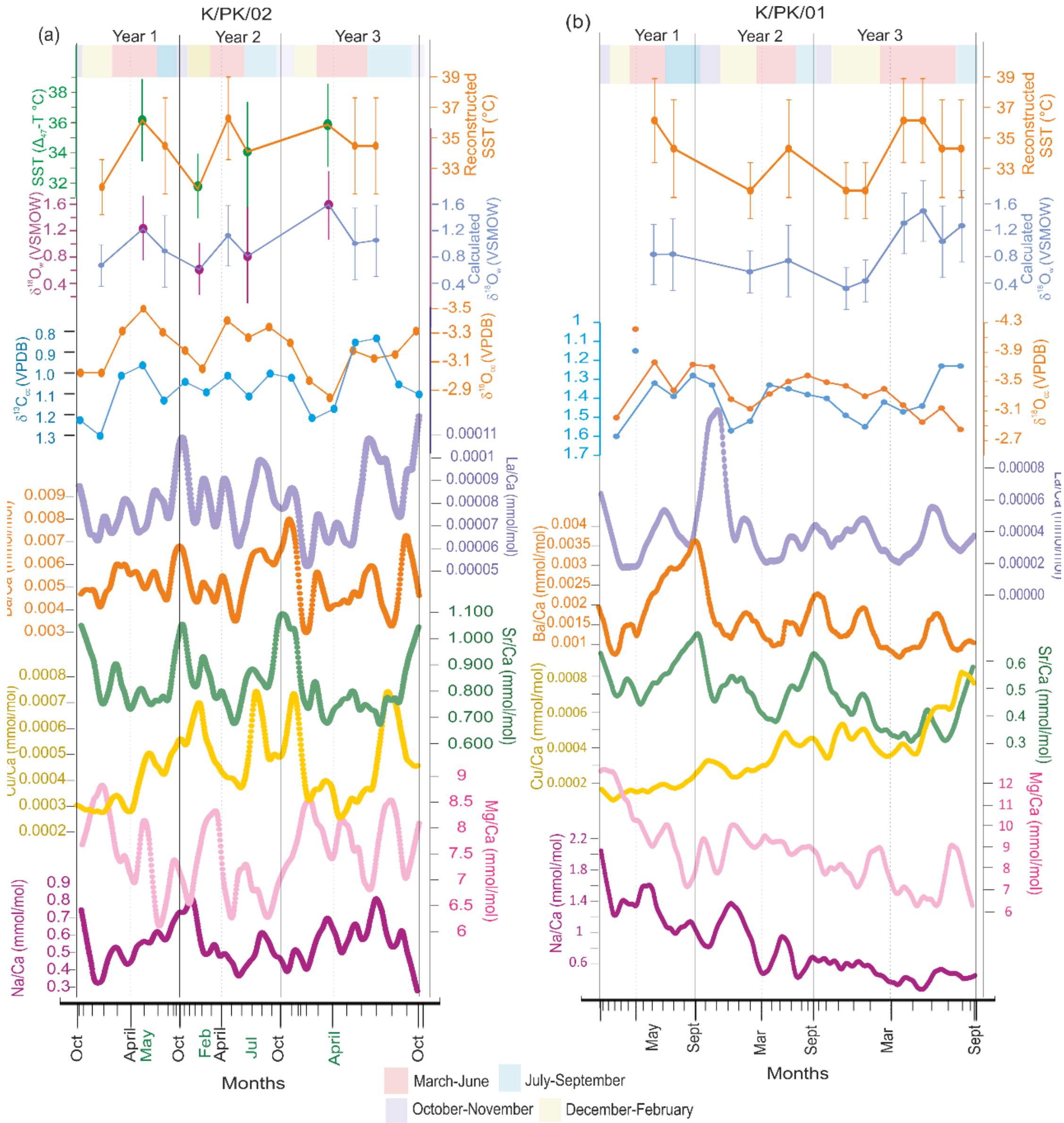

Figure 7. Trace element-to-Ca ratio profiles smoothened (LOWESS interval 0.1) along the growth axis of K/PK/02 and K/PK/01 are plotted together along the growth axis along with shell-chronology and stable isotope data, estimated Δ_{47}-T (red dots with 95% CI) and $\delta^{18}O_w$ (violet dots with 95% CI) values. Clumped isotope derived temperature estimates for the respective months along the shell chronology of K/PK/02 and K/PK/01 are shown as orange dots with 95% CI, with the corresponding calculated $\delta^{18}O_w$ ($f(D_{47}\text{-}T, \delta^{18}O_{cc})$) values shown as blue dots.

Lines 598-601:

Seasonal variability in shell-recorded LILE concentrations, likely driven by rainfall and freshwater influx, together with generally low REE concentrations and their sharp increase during the higher precipitation months (Fig. 7), consistent with episodic terrestrial freshwater input, provides supporting evidence for seasonal hydroclimatic variability in the lagoonal system.

Overall, this manuscript shows potential but focusses on conclusions that lack data to support it and has limited explanations on their used assumptions.

Response

We have thoroughly revised the manuscript in response to all comments and suggestions from Reviewer 1 and Reviewer 2 and the comment from the scientific community. We have incorporated a shell-growth chronology and used this framework to place conventional stable-isotope data points within the multiannual growth records of the two specimens. We have also strengthened the discussion of our methodological assumptions and preservation criteria. Importantly, we have substantially moderated our interpretations and refrained from making claims beyond what is directly supported by the integrated proxy data.

Line-specific comments

Line 1: the title is misleading as you only consider one shell for your conclusions.

Response: In the revised manuscript, our interpretations are based on a multi-proxy approach using two specimens, K/PK/01 and K/PK/02, integrating conventional stable isotopes, clumped isotope, trace-element profiles, and shell-growth chronology. As stated above, we have substantially moderated our conclusions to ensure that they remain commensurate with the available data. Accordingly, we have revised the title to:

Sustained high temperatures and seasonal hydroclimate variability recorded in the middle Eocene oyster shells from the tropical western Indian margin

Line 13-14: I would change the comma to after "understood"

Response: Placed the comma after understood.

Following adjustments in the manuscript, the opening lines of abstract are as follows:

The late-middle Eocene (Bartonian) marks a transition from the Middle Eocene Climatic Optimum (MECO) toward progressive global cooling, accompanied by declining atmospheric CO_2 concentrations. The impact of this transition on tropical seasonality remains poorly understood, mainly due to the paucity of suitable seasonal proxies coupled with climate simulations.

Line 20-22: you are misleading the reader here, since you only consider one specimen to be reliable, even though you measured three for trace elements. Clearly state that you only consider one specimen for your conclusions or readjust your focus to an exploration/analysis of *Pycnodonte* preservation.

Response: In the revised manuscript, much more focus is engaged in both the well-preserved specimens K/PK/01 and K/PK/02. So, the interpretation is based on both these specimens. We have discussed this point in detail in the responses to your first to third feedback.

Line 29: observed in what? The model or oysters? That is unclear.

Response: The observation is based on combined result of proxy-based result which is compared with the CESM results.

Observed climatic and seasonal variability in geochemical signature from the oyster shell, supported by the climate model are comparable to the underlying MECO oyster record, despite the early Bartonian short-term warm conditions and the gradual decline in pCO_2 toward the late Bartonian, suggesting a limited sensitivity of equatorial climate to atmospheric CO_2.

Line 30: hyperthermals are defined as peak warmings above the normal background temperature, so this is misleading in naming an entire period of hyperthermal conditions. Overall warmth and frequent hyperthermals did occur but were not constant.

Response: Thank you for pointing this out. We have updated it in the manuscript. Please see the manuscript extract to the last comment.

Line 47: I would change the word deciphering as you cannot decipher between multiple subjects. I imagine you mean decipher between the effects of/impact of these drivers.

Response: We presume, you indicated to line 37. As we understand that from our results and your feedback, monsoon signal cannot be interpreted thus we have modified the opening paragraph and deleted the sentence altogether.

The Eocene witnessed a progressive transition from greenhouse to cooler climate conditions, driven in part by declining atmospheric pCO_2, but punctuated by transient warming episodes such as the Middle Eocene Climatic Optimum (MECO; ~40 Ma), when a rise in pCO_2 temporarily reversed the long-term cooling trend (CenCO_2PIP Consortium, 2023; Westerhold et al., 2020). Against this backdrop of global climatic change, the South Asian summer monsoon (SAM) system was developing during the middle to late Eocene, influenced by Significant tectonic and palaeogeographic changes in Asia (Huber and Goldner, 2012; Dimri et al., 2016; Tardif et al., 2020, 2023; Mitra and Halder, 2024; Abhik et al., 2026 and references therein). However, its timing and character remain debated, with evidence ranging from a fully developed monsoon by the late Eocene to an arid northern India with seasonal variability driven by Intertropical Convergence Zone (ITCZ) migration during 42-38 Ma (Huber and Goldner, 2012; Licht et al., 2014; Tada et al., 2016; Tardif et al., 2020, 2023). Understanding the evolution of seasonality in South Asia under these rapidly changing climatic and ongoing monsoon development therefore remains an important question.

Line 49-51: the order of this sentence is confusing, consider moving “the hydrological cycle” earlier in the sentence before the comma.

Response: Removed the comma.

Stable isotope sclerochemistry of fossil shells is a powerful tool for reconstructing sub-annual climate, as growth-increment-resolved carbonate records capture changes in temperature and hydrological cycle.

Line 51, 54: is there a reason you first mention oyster and then bivalves, since the former is a subgroup of the latter?

Response: The first mention should have been ‘bivalve’. It was a mistake. Changed it and subsequently included “(a subgroup of Bivalvia)”, when mentioned the first time “Oyster”.

Line 55-56: Bivalve shells exhibit cyclical, seasonal patterns…….

Line 60-63: The geochemical behaviour of rare earth elements (REE) investigated in fossil oyster (a subgroup of Bivalvia) shells suggest that REE signatures can be preserved and potentially reflect palaeoenvironmental conditions, but these patterns can be affected by diagenetic overprints and biological fractionation (Akagi and Edanami, 2017; Briant et al., 2021; Valdés-Vilchis et al., 2021; Mouchi et al., 2020; Barrat et al., 2023).

Line 59: is a very long sentence, split up after the "for example".

Response: We have split the sentence. See line 60-63 and 63-65.

Line 63-65: Studies show that REE patterns in *Crassostrea gigas* reflect environmental variations, while REE incorporation in *Ostrea edulis* appears largely unaffected by environmental factors (Mouchi et al., 2020).

Line 146: should be "one half was prepared" not halves.

Response: Corrected.

The specimens were cleaned, dissected using a diamond coated saw, and one half was prepared as 5 mm thick sections following the methodology outlined in Mitra et al. (2025).

Line 147: 05 mm doesn't make sense, just 5 mm would be clearer.

Response: Corrected.

Line 164: what is the resilifer region? Non-experts might not be familiar – explain or indicate on figure.

Response: We have included a vector image representing the pycnodonts and pointing out to its resilifer region in Figure 2a. A close-up image of pycnodont resilifer (Fig. 2b) is also included.

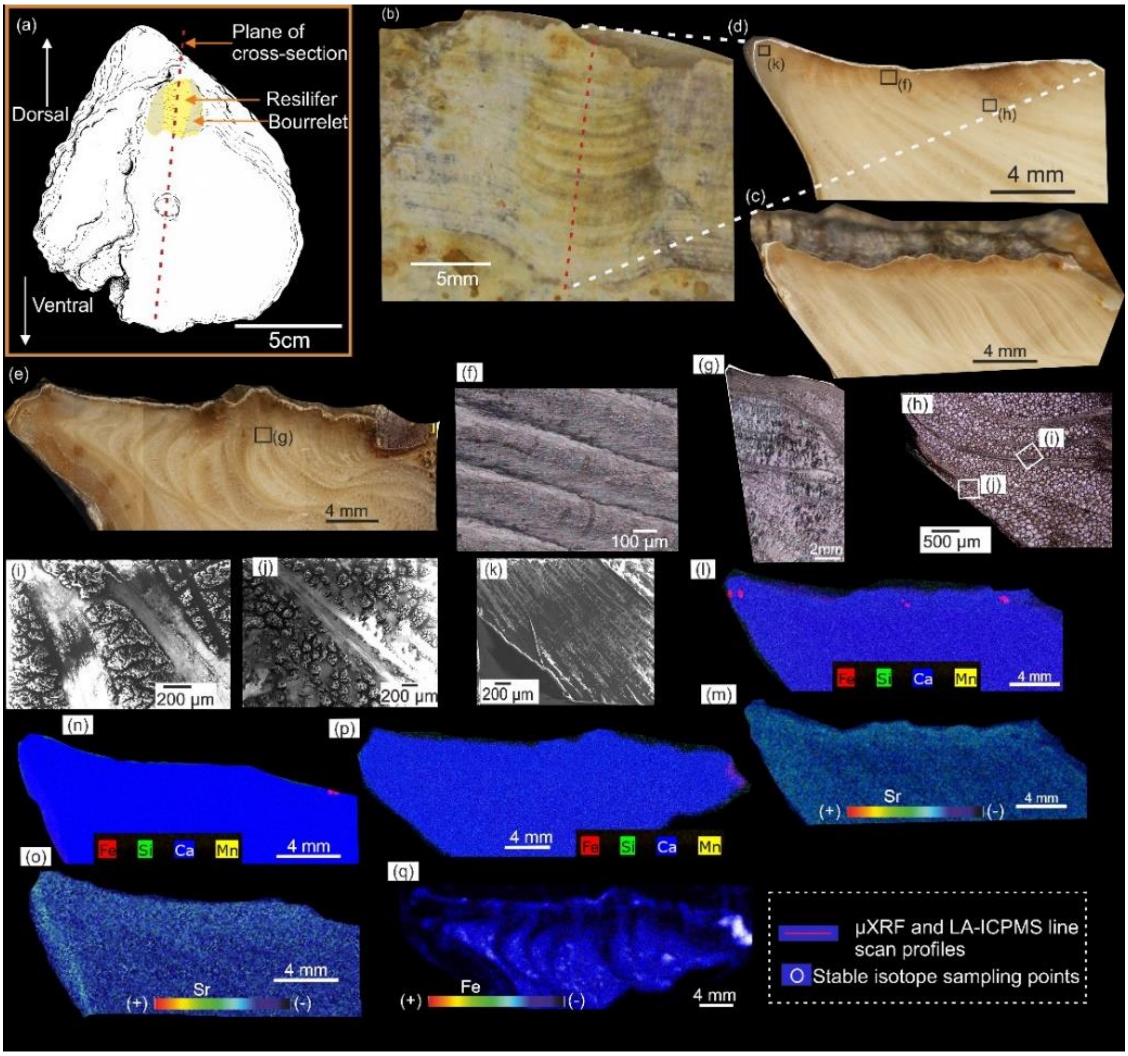

Figure 2. (a) Schematic diagram of *Pycnodonte kachchhensis* with plane of cross-section marked by dashed red line; Resilifer and bourlette makes the ligamental zone; (b) analysed ligamental region of K/PK/02; (c-e) Cross-sectional photograph of the shell resilifers: (c) K/PK/01 (d) K/PK/02 and (e) K/Pk/03; (f-h) Thin section microscopic images: (f) Foliated calcite from the resilifer zone of K/PK/02; (g-h) Foliated and vesicular calcite in (g) K/PK/03 and (h) K/PK/02; (i-k) SEM images of foliated and vesicular calcite zones from K/PK/02; (l-q) µXRF scanning mapss of (l, n, p) Ca, Si, Mn and Fe (colour coded) and (m, o, r) elemental heat map of (i,m) K/PK/01, (n,o) K/PK/02 and (p,q) K/PK/03.

Line 200: you have four Δ_{47} datapoints, state that clearer here as the wording is confusing. How it is written now, you have a lot of equidistant datapoints along the entire shell that you measured for $\delta^{13}C$ and $\delta^{18}O$ but not for Δ_{47} following your Table 3. Did you pool together equidistant samples then state this, but this will significantly change your story of what months and seasons you define?

Response: Corrected. Additionally, shell growth model provided season and month estimates.

Clumped isotope thermometry was performed on four samples, selected to represent the highest to the lowest values of $\delta^{18}O_{cc}$ from the resilifer region of K/PK/02 and each Δ_{47}-T is based on 9-11 replicates to provide robust temperature estimates at the 95% CI.

Line 210: why the ICDES90 scale, I-CDES is defined and reported to the 90°C reaction temperature so the specific indication of I-CDES90 is not needed. And you did not measure dual clumped, which is often denoted as CDES90.

Response: Corrected.

The $D_{47\text{-raw}}$ data were processed with simultaneously measured ETH-1, ETH-2 and ETH-3 standards, from which an empirical transfer function (ETF) was determined by plotting their raw values versus their published accepted values at the I-CDES scale (Bernasconi et al., 2018; 2021).

Line 337: you use "which" twice, one needs to be "that".

Response: Adjusted.

Notable exceptions include trace elements such as Na, Ti, Ni and Zn, which show some degree of variability that can be an effect of dissolution and reprecipitation (Fig. S4; Brand and Veizer, 1980; Casella, 2019).

Line 340: were any clumped isotope measurements performed on the other two specimens to confirm your suspicions of diagenesis? Especially since you only have one specimen that you trust vs two you don't i.e. more "diagenetic altered" specimens than not, it would make more sense to pivot part (or maybe even most) of your story to the potential effects of diagenetic alterations. Or at least have a more significant part exploring this, as this is still interesting to the clumped community (i.e. diagenetic effects, potential burial temperatures, or preservation analyses).

Response: We fully agree that analysing data points from potentially diagenetically altered zones could provide valuable constraints for future clumped isotope studies and contribute to a better understanding of diagenetic effects on clumped isotope temperature estimates. However, in the present study, we have followed established preservation criteria from the published literature and restricted our clumped isotope analyses to the specimen K/PK/02 that show the strongest geochemical evidence for pristine preservation, characterised by consistently low concentrations of secondary elements, particularly Fe and Mn (<800 µg/g). This approach minimises the potential influence of diagenetic alteration on the reconstructed temperatures and ensures that our interpretations are based on the best-preserved carbonate material available.

Line 389-399:

K/PK/01 contains three Fe-enriched zones along the first transect and at ~2 mm, high Fe concentrations of >800 µg/g coincide with elevated Si (>0.1 wt%) and an exceptionally low $\delta^{18}O_{cc}$ value (4.21‰; Fig. 3), supporting Fe enrichment as an indicator of local diagenetic modification. A similar association of high Fe and Si with low Ca occurs across a substantial section of K/PK/03, further supporting this interpretation. However, the absence of comparable Si and $\delta^{18}O_{cc}$ anomalies at ~8 mm of K/PK/01 despite elevated Fe indicates spatial heterogeneity, and thus the >800 µg/g Fe threshold is best regarded as a conservative screening criterion rather than a universal alteration threshold. In contrast, K/PK/02 exhibits consistently low Fe and Mn concentrations (<300 µg/g) throughout the analysed profile. Given the potential for spatially heterogeneous diagenetic alteration indicated by the Fe-rich zones in K/PK/01 and the criteria established in previous studies, K/PK/02 was therefore selected for clumped isotope (Δ_{47}) analysis to minimise the potential influence of diagenesis.

Line 346: "reflects" should be singular.

Response: Corrected.

In the underlying Harudi Formation, a sharp negative carbon isotope excursion (CIE: ~2 ‰) coinciding with the lowest taxon range zone of SBZ17 and E11 biostratigraphic interval has been interpreted to reflect the MECO event at ~40 Ma (Fig. 5).

Lines 347-348: two things; one, you are comparing $\delta^{13}C$ signals from foram carbonate vs organic carbon, how do you consider that to be comparable? Two, strong disagree that the MECO is not associated with a CIE, see (Spofforth et al., 2010 10.1029/2009PA001738; Sharma et al., 2024 10.5194/cp-20-935-2024; Mulch et al., 2015 10.2475/04.2015.02) for organic, benthic foraminifera, and bulk carbonate CIEs associated with the MECO.

Response: In the revised version, $\delta^{13}C_{org}$ signal of Kutch MECO is compared with $\delta^{13}C_{org}$ signatures from Ainsa Basin Spain, Bohay Basin China and Kutch Basin India. It was a mistake from our side, that we mentioned that MECO is not associated with CIE. We have corrected it. Accordingly, we have also included the supporting references in the figure.

Records from terrestrial to marginal marine settings like Bohai Bay Basin of China (CIE: ~1.7‰), Ainsa Basin of Spain (CIE: ~1‰), Belluno Basin in Italy, the Kutch Basin of India document negative excursions of ~1-2 ‰ in $d^{13}C_{org}$ (Spofforth et al., 2010; Khanolkar et al., 2017; Ma et al., 2024; Sharma et al., 2024).

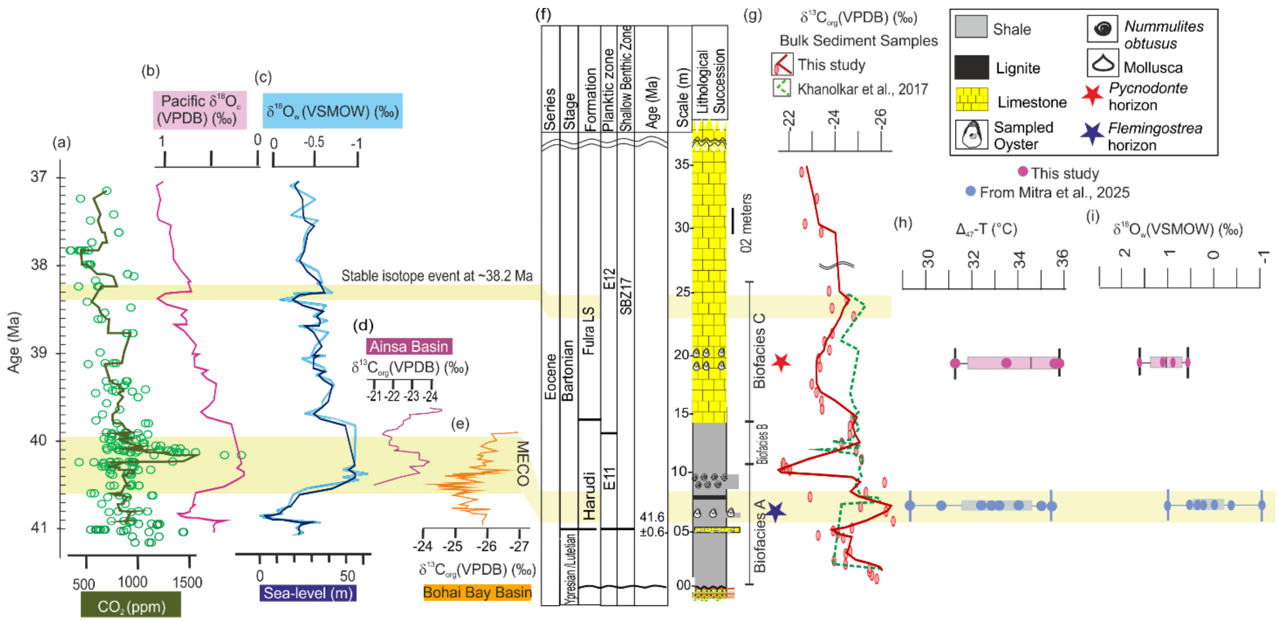

Figure 5. (a) Atmospheric pCO_2 estimates (symbols) with five-point moving average (after CenCO$_2$PIP Consortium, 2023) (b-c) Records from the Pacific Ocean cores with five-point moving average (after Miller et al., 2020): (b) Pacific $\delta^{18}O_{cc}$ stratigraphy of the Eocene based on *Cibicidoides* spp., (c) Sea level and $\delta^{18}O_w$ values; (d-e) $\delta^{13}C_{org}$ stratigraphy from Ainsa Basin, Spain and Bohai Bay Basin of China; (f) Lithostratigraphic section of the Bartonian sequence in the Kutch Basin, with (g) bulk sediment $\delta^{13}C_{org}$ stratigraphy with three point moving average from this study along with $\delta^{13}C_{org}$ stratigraphy from Khanolkar et al., 2017, (h) estimated temperatures and (i) $\delta^{18}O_w$ values from the respective stratigraphic horizons of early Bartonian *Flemingostrea* (Mitra et al., 2025) and late Bartonian *Pycnodonte* (this study).

Line 373: "on average".

Response: Corrected.

This shift is associated with contrasting $\delta^{13}C_{org}$, $\delta^{18}O_w$ and $\delta^{18}O_{cc}$ signatures between the early and late Bartonian (Figs. 5, 6a; Mitra et al., 2025), the late Bartonian dataset reveals on average approximately 1 ‰ higher $d^{18}O_w$ (Fig. 5h-i).

Line 375: "relatively much higher" sounds weird, either relatively higher or much higher.

Response: Corrected.

Based on benthic foraminifera Cibicidoides spp., which has a carbonate δ18Occ value of -0.5 to -1.5 ‰ (Fig. 5b, Lear et al., 2004; Cramer et al., 2011), the tropical seawater δ18Ow value during the Bartonian (0 to -1 ‰) was lower than in modern times (0.2-0.5 ‰) in a much higher pCO2 condition (Fig. 5a-b; Schmidt et al., 1999; Tripati et al., 2014).

Line 380: it is from one specimen that reflects local conditions, how variable is $\delta^{18}O_{sw}$ in the modern day, comparable enough to make such a statement?

Response: We have discussed the seasonal variability of $\delta^{18}O_w$ in detail in Section 5.5.3, "Comparison with modern seasonality."

Lines 647-658

While $\delta^{18}O_w$ of the Arabian Sea, Bay of Bengal and the Indian Ocean today remain higher than river water throughout the year, coastal and lagoonal systems on the eastern India show strong monsoonal $\delta^{18}O_w$ depletion linked to freshwater influx (Fig. 10; Singh et al., 2010; Colonese et al., 2017). The monsoonal rainfall in India exhibits significantly lower $\delta^{18}O_w$ (-6 to -10 ‰) values, which results to markedly lower $\delta^{18}O_w$ of freshwater than marine (Rai et al., 2014; Jeelani et al., 2018). By analogy, the elevated $\delta^{18}O_w$ values observed in our study reflect climatic conditions comparable to the highly evaporative modern Gulf of Kutch with ~0.5 ‰ depletion of coastal seawater and ~1.0 ‰ depletion of river water near estuary during rainfall (Fig. 10). In the Bay of Bengal and Arabian Sea adjacent to Kerala, seasonal $\delta^{18}O_w$ variation is muted due to open marine condition (Fig. 10e-f). In Chilika, a brackish coastal lagoon in eastern India, pronounced seasonal variability in $\delta^{18}O_w$ is evident, with values decreasing from 0.23‰ in April to -2.14 ‰ in September, consistent with substantial monsoonal freshwater input (Singh et al., 2010). Moreover, the Eocene values of Kutch suggest an even more restricted environment, as they exceed both present-day and contemporaneous marine $\delta^{18}O_w$ levels comparable to modern lagoons where $\delta^{18}O_w$ is higher than the surrounding ocean water (Blamart et al., 2002).

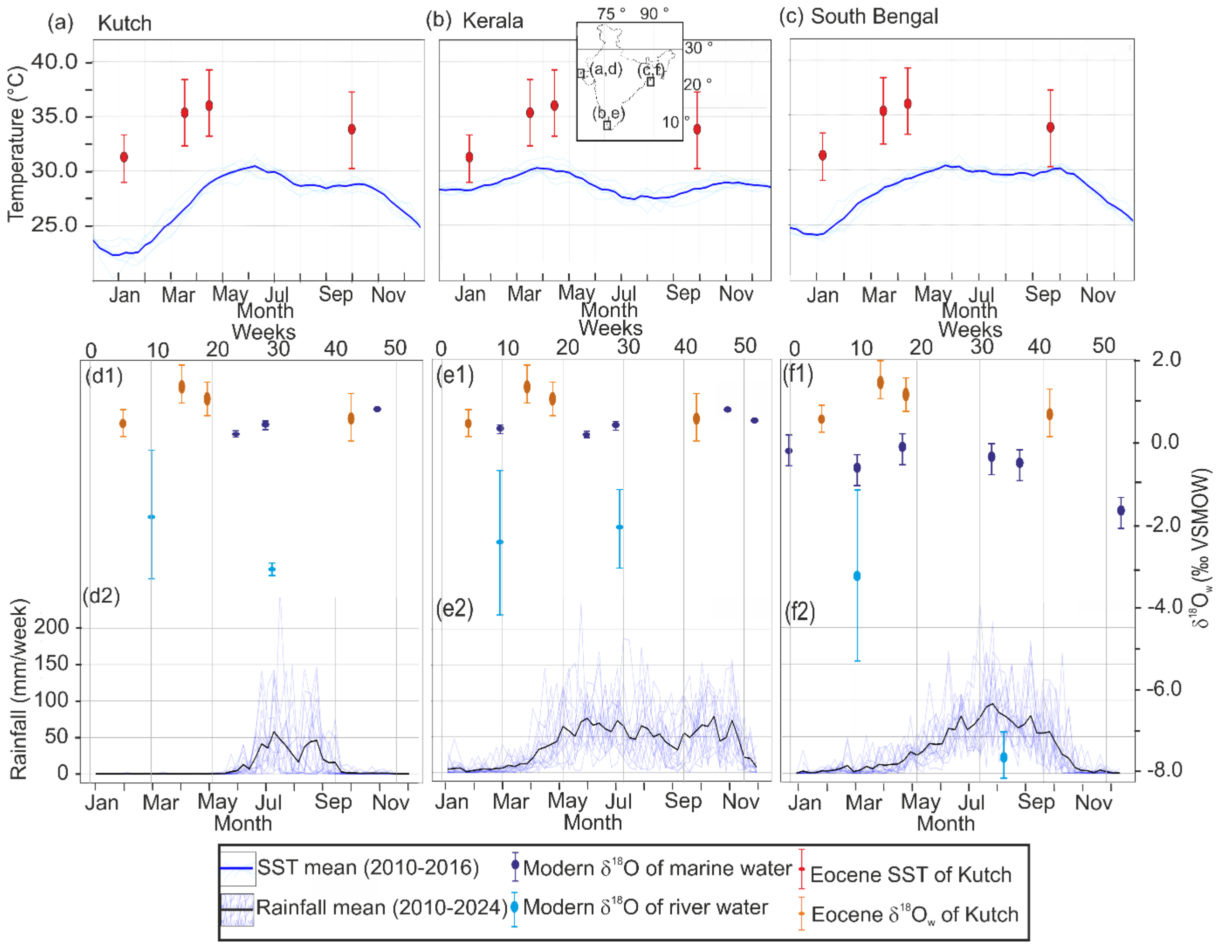

Figure 10. Late Bartonian sea-surface temperature (SST) and $\delta^{18}O_w$ are compared with modern SST, surface air temperature (SAT), and $\delta^{18}O_w$ of river water (below 80 m altitude) and marine water. Panels (a-c) show comparisons of Bartonian SST (Δ_{47}-T) with modern SST from (a) Kutch, (b) Kerala, and (c) southern Bengal. Late Bartonian $\delta^{18}O_w$ (*f* (Δ_{47}-*T*, $\delta^{18}O_{cc}$)) values are compared with seasonal marine and river-water $\delta^{18}O_w$, from (d) Kutch, (e) Kerala, and (f) southern Bengal,India: regions that experience the modern monsoon with differing intensity and timing. Source: Modern rivers- Kirkels, 2020; Modern Ocean: LeGrande and Schmidt, 2006.

Line 431: Your entire study depends on the definition of seasons within your one specimen. However, how you define your seasons is seemingly subjective and not robust. You compare your four datapoints to the CESM seasonal temperatures, but you automatically start in Jan, is there evidence that growth started in Jan and not in spring or summer as is the case with other molluscs? Especially as you have two May datapoints with completely opposite $\delta^{18}O$ values, so they are seemingly from opposite seasons. Indeed, your $\delta^{13}C$ has a much clearer sinusoidal pattern and suggests your second year should be shifted by several months, i.e. your 2nd year May/June has the same values as 1st year Jan/Feb.

Response: In the revised manuscript, we have clarified the methodological framework used to assign the seasonal positions to the isotope measurements:

a) We first constructed an ontogenetic growth model for K/PK/01 and K/PK/02 using the $\delta^{18}O_{cc}$ and high-resolution Sr/Ca profiles, implemented through ShellChron (de Winter, 2022).

b) The clumped isotope analysis (4 samples with 40 replicates) yielding the highest temperature was used as the seasonal reference point and assigned to May, corresponding to the May-June interval identified as the warmest period in both the CESM simulations for the Eocene and the modern seasonal climatology.

c) The corresponding monthly positions of the remaining clumped isotope measurements in K/PK/02 were then determined from the growth model.

d) The inverse relationship between $\delta^{18}O_{cc}$ and temperature is supported by the published literature and is also evident in three of the clumped-isotope-constrained points from K/PK/02. Following this relationship, the lowest $\delta^{18}O_{cc}$ value in K/PK/01 was used as the corresponding warm-season reference point.

e) The remaining monthly positions in both specimens were subsequently assigned according to the ShellChron-derived growth model.

f) We acknowledge that the absolute calendar-month assignments carry some uncertainty. However, the relative temporal spacing between successive sampling positions is constrained by the growth model and therefore remains consistent even if the absolute seasonal alignment were shifted. Consequently, the interpretation of the seasonal pattern does not depend solely on the exact designation of an individual month name, rather the gap of months.

Based on this, the conventional stable and clumped isotope dataset falls in seasonal pattern, along with the trace elements.

The seasonal scale is revised and attached to this document **(Figure 7), as a response to your third feedback**.

Line 459: But your Ba/Ca is highest in the coldest CESM and your defined winter season, not spring. And the lowest values are not during your two warmest datapoints but the coldest.

Response: The revised growth model, together with the aligned clumped isotope temperature estimates and trace-element profiles, places the highest Ba/Ca values consistently around September-October. Our proxy-based reconstruction indicates an increase in the precipitation-to-evaporation balance from May-June onward, consistent with climate-model simulations indicating enhanced seasonal rainfall. The occurrence of the highest Ba/Ca values during September-October may therefore reflect enhanced freshwater and nutrient delivery to the coastal environment during the wetter season, potentially promoting increased marine productivity. This interpretation is also consistent with previous studies reporting elevated Ba/Ca and Sr/Ca associated with freshwater influx and enhanced terrestrial input.

Please see our response to the third feedback.

Line 475: But this is circular reasoning as the $\delta^{18}O_{sw}$ is defined using the $\delta^{18}O_{cc}$ and temperature from the same shell and are thus not independent variables.

Response: Thank you for pointing this out. We have removed the statement.

Line 509: are modern and Bartonian seasons comparable in how you defined them?

Response: The modern and Bartonian seasons are not considered directly equivalent in terms of their absolute temperature ranges or seasonal definitions. In the revised manuscript, we therefore use the modern names of the months primarily as a month analogue for the timing and relative sequence of seasonal changes, rather than assuming identical seasonal conditions with the Bartonian.

In the Bartonian record, reconstructed temperatures range from approximately 31-36 °C, with $\delta^{18}O_w$ values of ~0.5-1.6 ‰. The growth chronology indicates systematic changes in the relationship between temperature and $\delta^{18}O_w$ through the year: the warmest interval is characterised by high temperature (~36 °C) and relatively high $\delta^{18}O_w$ (mean ~1.2 ‰), followed approximately two months later by moderately high temperature (~34 °C) and lower $\delta^{18}O_w$ (mean ~0.9 ‰), followed by still lower temperatures and $\delta^{18}O_w$ (mean ~0.4 ‰) after approximately nine months. These recurring relationships provide the basis for our seasonal interpretation.

We use May as the reference warm-season month because the highest reconstructed temperature corresponds to the warmest interval in both the Eocene CESM simulation and the modern seasonal climatology. In modern India, the major seasonal divisions are summer (March-June), monsoon (July-September), post-monsoon (October-November), and winter (December-February). Although the absolute SST range in the modern setting (~23-30 °C) is substantially lower than that reconstructed for the Bartonian (~31-36 °C), the relative seasonal temperature progression and the coupling between temperature and hydrological variability provide a useful basis for comparison.

The $\delta^{18}O_w$ variations further indicate seasonal hydroclimatic variability in the Bartonian record. In the modern western Indian coastal region, rainfall is strongly concentrated during the summer monsoon, whereas the winter months are comparatively dry. The occurrence of relatively lower $\delta^{18}O_w$ values during cooler intervals in our Bartonian record, supported by the climate-model simulations, suggests that seasonal precipitation was not restricted exclusively to the warmest interval and four months of a year. We have discussed this comparison in Lines **649-657**. Thus, we have clarified that the modern seasonal framework is used as a comparative reference for the relative seasonal progression, rather than as a direct one-to-one definition of Bartonian seasons. We have also moderated the terminology accordingly in the revised manuscript.

The segment of primary submission line 509; Lines 610-621:

Higher rate of precipitation than evaporation in June-July is marked by a decline in $\delta^{18}O_w$ to 0.4 - 0.8 ‰, complying with the model output. Because our proxy record does not cover September-December, the specific hydroclimatic response of the basin during these months cannot be directly assessed. Though, outside the summer and monsoon interval, CESM simulations indicate moderate precipitation even in modern winter months (December-February) in the Bartonian Kutch (Figs. 8b, 9), but that does not completely explain such lower value of $\delta^{18}O_w$ in January-February (0.00 - 0.6‰: Mean $\delta^{18}O_w$: 0.4±0.2 ‰ 1SD). The relatively lower value of estimated SST (Δ_{47}- T: 31°C) during this interval likely caused reduced evaporation, which combined with moderate rainfall resulted in lower $\delta^{18}O_w$ values. The climate-model and earlier studies indicate the open northern seaway between India and Eurasia as a probable source of moisture, contributing to precipitation till the early Eocene in December-February months (Tardif et al., 2023; Meijer et al., 2024; Akhmetiev et al., 2012; Wadood et al., 2021; Montheil et al., 2026; Figs. 9a-b, S7). Thus, the $\delta^{18}O_w$ record suggests a seasonal hydrological regime in which evaporation dominated during the warmest months, whereas precipitation became dominant to evaporation as temperatures declined.

Lines 671-683

In modern Kutch, as well as during the pre-industrial period, monsoon rainfall is largely confined to July-September (Figs. 8b, 10; Funk et al., 2015). In contrast, southern Bengal receives precipitation from the summer to the post-monsoon season in recent times. Modern Kerala experiences an extended annual rainfall season, with a secondary rainfall maximum toward the end of the year associated with the southward retreat of the monsoon and moisture transport from the Bay of Bengal by northeasterly winds (Figs. 8b, 9, and 10e; Sahadudheen et al., 2026). This highlights the role of land-sea configuration in modulating regional rainfall patterns, which may have been particularly important in Eocene India, when the palaeogeographic configuration (Montheil et al., 2026), including an open northern seaway, differed markedly from that of the present day. In our record, the occurrence of lower $\delta^{18}O_w$ values approximately two and nine months after the peak warm-month conditions suggest an extended and seasonally complex hydroclimatic regime distinct from that of modern Kutch, but with some similarities to the rainfall pattern of present-day Kerala. Thus, although a proto-monsoonal system likely existed in the late Bartonian Kutch Basin, its seasonal structure cannot be fully resolved from the available proxy record of this study. Nevertheless, the evidence suggests that precipitation was not confined to the four-month seasonal window characteristic of the modern north Indian monsoon.

Line 512: what are the ITCZ dynamics in relation to what is observed for these CESM model simulations?

Response: We have reorganised this section in the revised manuscript, as outlined in our response above (Lines 610-621). We have removed the discussion of ITCZ migration from the revised interpretation. Based on our proxy results, we consider that the available data do not provide sufficient constraints to determine the seasonal migration or position of the ITCZ. We have therefore avoided attributing the reconstructed seasonal hydroclimatic variability to ITCZ migration and have restricted our interpretation to the seasonal signals directly supported by the proxy data.

Line 531: although you just have four datapoints from one specimen.

Response: We have removed that statement. We have cited published literatures, which states the existence of the sea-way in the North of India. We addressed the issue in line 606-609; 613-620:

The climate-model and earlier studies indicate the open northern seaway between India and Eurasia as a probable source of moisture, contributing to precipitation till the early Eocene in December-February months (Tardif et al., 2023; Meijer et al., 2024; Akhmetiev et al., 2012; Wadood et al., 2021; Montheil et al., 2026; Figs. 9a-b, S7).

5.5.2 Comparison with the early Bartonian

Our proxy records indicate limited change in seasonal temperature variability that remain weak from the early to late Bartonian, with comparable temperature ranges of 29-36 °C and 31-36 °C, respectively (Figs. 5h, 6) and minor cooling (ΔT: 3-5 °C) during months of lower $d^{18}O_W$ (Figs. 6, 7a-b; Mitra et al., 2025). Despite atmospheric pCO_2 being substantially higher during the MECO (~4xPIC) compared to the late Bartonian (~2-3xPIC; Fig. 5a; Henehan et al., 2020; $CenCO_2PIP$ Consortium, 2023), model simulations and proxy-based earlier studies show that a reduction in pCO_2 from 1120 to 560 ppm had minimal influence on tropical seasonality vis-à-vis equatorial India with maximum effects on the northern hemisphere mid to high latitude seasonality and monsoons (Toumoulin et al., 2022; Tardif et al., 2023; Meijer et al., 2024).

Line 535: it just shows variability in one of your specimens though.

Response: As mentioned in the last response, we have removed this statement as well.

Line 535: do lagoons have strong $\delta^{18}O_{sw}$ fluctuations if the organism is always fully submerged and below the wavebase?

Response: We agree with you, that the seasonal $\delta^{18}O_w$ fluctuation signal will be dampened if the organism is continuously under wavebase, in comparison to organism which seasonally lives over the wavebase and in some seasons, under the wavebase.

Thus, we have deleted the statement in the revised manuscript.

Line 545: the start of this sentence reads weird, we investigate how to explain – rewrite.

Response: We have revised the sentence.

Line 628: We investigate the plausible mechanisms to explain the estimated elevated $\delta^{18}O_w$ values relative to typically lower values in modern monsoons.

Line 551: here you should make clear that this precipitation signal you are describing comes from the river water in that region, if you reference to Figure 10.

Response: We have revised the sentence with reference to figure 10 and added the following sentences.

Line 651-656:

By analogy, the elevated $\delta^{18}O_w$ values observed in our study reflect climatic conditions comparable to the highly evaporative modern Gulf of Kutch with ~0.5 ‰ depletion of coastal seawater and ~1.0 ‰ depletion of river water near estuary during rainfall (Fig. 10). In the Bay of Bengal and Arabian Sea adjacent to Kerala, seasonal $\delta^{18}O_w$ variation is muted due to open marine condition (Fig. 10e-f). In Chilika, a brackish coastal lagoon in eastern India, pronounced seasonal variability in $\delta^{18}O_w$ is evident, with values decreasing from 0.23‰ in April to -2.14 ‰ in September, consistent with substantial monsoonal freshwater input (Singh et al., 2010).

Line 557: what are the Eocene SST and SAT estimates here?

Response: We had made this statement entirely based on the CESM simulation results of the Eocene. As we do not have proxy-based data of SAT from this study, we refrain from making this comment in the revised manuscript.

Line 559: what do you define as summer and winter as there are two relative warm peaks and two relative colder periods?

Response: We have removed the previous statement referring to surface-air temperature (SAT) and SST gradient comparison, as SAT is not directly reconstructed from our proxy data. In the revised manuscript, the terms summer and winter are used only in reference to the modern seasonal framework and the corresponding Eocene CESM simulation, with March-June designated as the summer/warm season based on the clumped isotope temperature constraints and the CESM simulation. The subsequent, relatively warm interval occurs during the post-monsoon period, when rainfall decreases, and is broadly consistent with the seasonal temperature recovery observed in the modern climate of India (Figure 10).

Line 562: is this shown in a,b,c as your blue line? It should also be singular as it is only one specimen.

Response: We have revised the sentence and the figure 10. We think it is more legible now.

Modern Kutch, Kerala and southern Bengal exhibit ~2 °C SST decline during the monsoon, a pattern mirrored in our Eocene record where temperature drops coincide with lower $\delta^{18}O_w$ values (Fig. 10).

Line 572: is there a significant difference between modern and pre-industrial in this sense, since you only show data from 2010-2016 in Fig. 10 and model simulations in Fig. 8? Also, during the monsoon months of July-Sept in Fig. 8, the difference between PI and Eocene is only 50 mm (only 1/6th of the overall precipitation signal) but much larger in the preceding and following months. Consider rewording or adjusting what you mean with magnitude.

Response: We have revised the statement.

In modern Kutch, as well as during the pre-industrial period, monsoon rainfall is largely confined to July-September (Figs. 8b, 10; Funk et al., 2015).

Line 580: consider adding "reduced temperature and inferred hydrology record".

Response: During the revision, we recognised that the seasonal SST difference between the warm and cool intervals in the Eocene (ΔT ~5 °C) is not substantially different from that observed in the modern record (ΔT ~7 °C). We have therefore revised the discussion of seasonal variability accordingly and modified the concluding statements accordingly.

Thus, although a proto-monsoonal system likely existed in the late Bartonian Kutch Basin, its seasonal structure cannot be fully resolved from the available proxy record of this study. Nevertheless, the evidence suggests that precipitation was not confined to the four-month seasonal window characteristic of the modern north Indian monsoon.

Lines 589-596: you only consider one shell with one datapoint in another year so I would give the opening sentence a lot more nuance. Further, you base this concluding paragraph on your one specimen, even though most of it is describing the model simulation results. Please rewrite this section and adjust the focus.

Response: We have revised the opening statement.

Lines 667-670: Proxy-based reconstruction from the multi-year archive of the pycnodont shells, supported by climate model simulations, reveal small seasonal temperature difference (ΔSST: ~5 °C: 31-36 °C) comparable to modern western India (ΔSST: ~7 °C: 23-30 °C). The region likely maintained generally more extreme sea-surface temperatures than the present Gulf of Kutch, with rainfall-driven cooling events associated with typical reduced evaporation for at least twice a year with a gap of ~7-8 months.

Figure and table comments

Table 3: Δ_{47} is classified as IDES and not ICDES and $\delta^{18}O_w$ and not $\delta^{18}O_{sw}$ in the description.

Response: We have corrected this, and maintained I-CDES throughout the manuscript.

Figure 5: you compare your $\delta^{13}C_{org}$ record to that of Khanolkar et al. (2017) and both have a CIE close to each other at 5 m and similar trend around 25 m. Are these not the same? How did you correlate their record to yours if your y-axis in this case is m and not age?

Response: We have matched the record of our $\delta^{13}C_{org}$ with that of Khanolkar et al. (2017) result from lithostratigraphy, bio-stratigraphic markers and the relative position of the marker beds like Coquina limestone, *Nummulitic obtusus* bed and Harudi-Fulra boundary (lines 404-411).

The CIE at ~25m is addressed properly in the revised manuscript. A record of $\delta^{18}O$ negative excursion at ~38.2 Ma is found from Pacific Ocean, which indicate a warming event. Our ongoing study also marks a ~3 °C temperature excursion in this interval. Thus, this CIE probably indicates a small warming event (Lines 420-429).

Lines 404-411:

Our $\delta^{13}C_{org}$ stratigraphy is compared with that of Khanolkar et al. (2017) using bio-stratigraphic markers and relative height from formation boundaries. Biofacies A corresponds to the grey shale to lower green shale of the Harudi Formation and is characterised by the first appearance of the coquina shell bed and the *N. obtusus* bed. Biofacies B encompasses the upper green shale of the Harudi Formation and is marked by the appearance of *Discocyclina* and the Harudi Formation-Fulra Limestone boundary. Biofacies C corresponds to the Fulra Limestone, where *Alveolina* and *Assilina* are dominant (Khanolkar et al., 2017). In addition to these biofacies markers, the relative stratigraphic positions of the CIEs with respect to the marker beds are considered to facilitate a direct comparison between the two chemostratigraphic records.

Lines 420-429:

The Fulra Limestone, conformably overlying the Harudi Formation, records a small (~1‰) negative $\delta^{13}C_{org}$ excursion at ~24 m above the Harudi Formation base. This may reflect a localised warming or regional oceanographic perturbation during the late Bartonian cooling, potentially correlative with the small equatorial Pacific $\delta^{18}O$ negative excursion at ~38.2 Ma (Borrelli et al., 2014). However, this correlation remains tentative given the absence of a globally synchronous late Bartonian warming event. An ongoing clumped isotope palaeotemperature reconstruction of the Fulra LS independently indicates a ~3°C warming broadly coincident with this horizon (Chaudhuri et al., under review). Otherwise, the Fulra LS has relatively higher $\delta^{13}C_{org}$ values comparative to early Bartonian units, consistent with the global trend of increasing $\delta^{13}C$ during the late Bartonian (Table 1; Fig. 5; Henehan et al., 2020; Ma et al., 2024). Consequently, the *Alveolina* wackestone interval, from where *P. kachchhensis* was collected, is interpreted to represents late Bartonian cooling phase based on relative chemostratigraphic position and biostratigraphic correlation (Fig. 5).

Figure 7: The $\delta^{18}O_{cc}$ does show a sinusoidal variability but your definitions of which season/month are which are not clear. Is there (a lack of) evidence for growth cessation? The highest $\delta^{18}O_{cc}$ in the second year does not coincide with your coldest temperature rather with one of the warmest.

Response: The figure has been revised and is also included in the response document. The fourth clumped isotope point of K/PK/02 corresponds to a high temperature and corresponds to high $\delta^{18}O_{cc}$ value. A similar pattern between the assigned months and the $\delta^{18}O_{cc}$ curve is observed in both specimens toward the end of their lifespans. During this interval, an inverse relationship between $\delta^{18}O_{cc}$ and $\delta^{13}C_{cc}$ is also evident. These observations and their implications have been addressed in the revised manuscript **(Fig. 7)**.

We have attached the revised figure in response to the third feedback.

Lines 523-536:

However, the fourth clumped isotope point (at 12mm of K/PK/02) records relatively high $\delta^{18}O_{cc}$ (-2.84 ‰) despite a high temperature (36 °C), coinciding with the highest $\delta^{18}O_w$ value (1.6‰). This decoupling demonstrates that $\delta^{18}O_w$ variability substantially modulated $\delta^{18}O_{cc}$ in addition to temperature. The neighbouring low $\delta^{18}O_{cc}$ value at 13 mm (-3.18‰) and its potential influence on the clumped isotope powder measurement at 12mm of K/PK/02, given their close spatial proximity, cannot be ruled out.

The January-February, April-May, and June-July intervals identified in the K/PK/01 and K/PK/02 shell chronologies were assigned temperatures from the independent clumped isotope averages of those months based on 9-11 replicates each.

Corresponding $\delta^{18}O_w$ values from those points (10 points of K/PK/01 and 5 points of K/PK/02) were calculated using the Kim and O'Neil (1997) equation ($\delta^{18}O_{w\ VSMOW}$ =[(1000+$\delta^{18}O_{cc}$)/exp{18.03/(D_{47}-T+273.15)- (32.42/1000)}]-1000) from the SST estimates (°C) and respective $\delta^{18}O_{cc}$ values (in VSMOW) along the shell transects. The water $\delta^{18}O_w$ and SST show a consistent inverse relation with $\delta^{18}O_{cc}$, whereas $\delta^{18}O_{cc}$ values show higher value to high SST and vice-versa during the final 4-6 months of growth for both of the shells (Fig. 7; Supplementary Table S3). The concurrent reversal between $\delta^{13}C_{cc}$ and $\delta^{18}O_{cc}$ suggests that this late-stage divergence is unlikely to be an effect of temperature alone and may instead indicate ontogenetic or physiological effects (Fig. 7; Mitchell et al., 1995).

Figure 9: indicate where your study site is.

Response: We have revised the figure and indicated the study site.

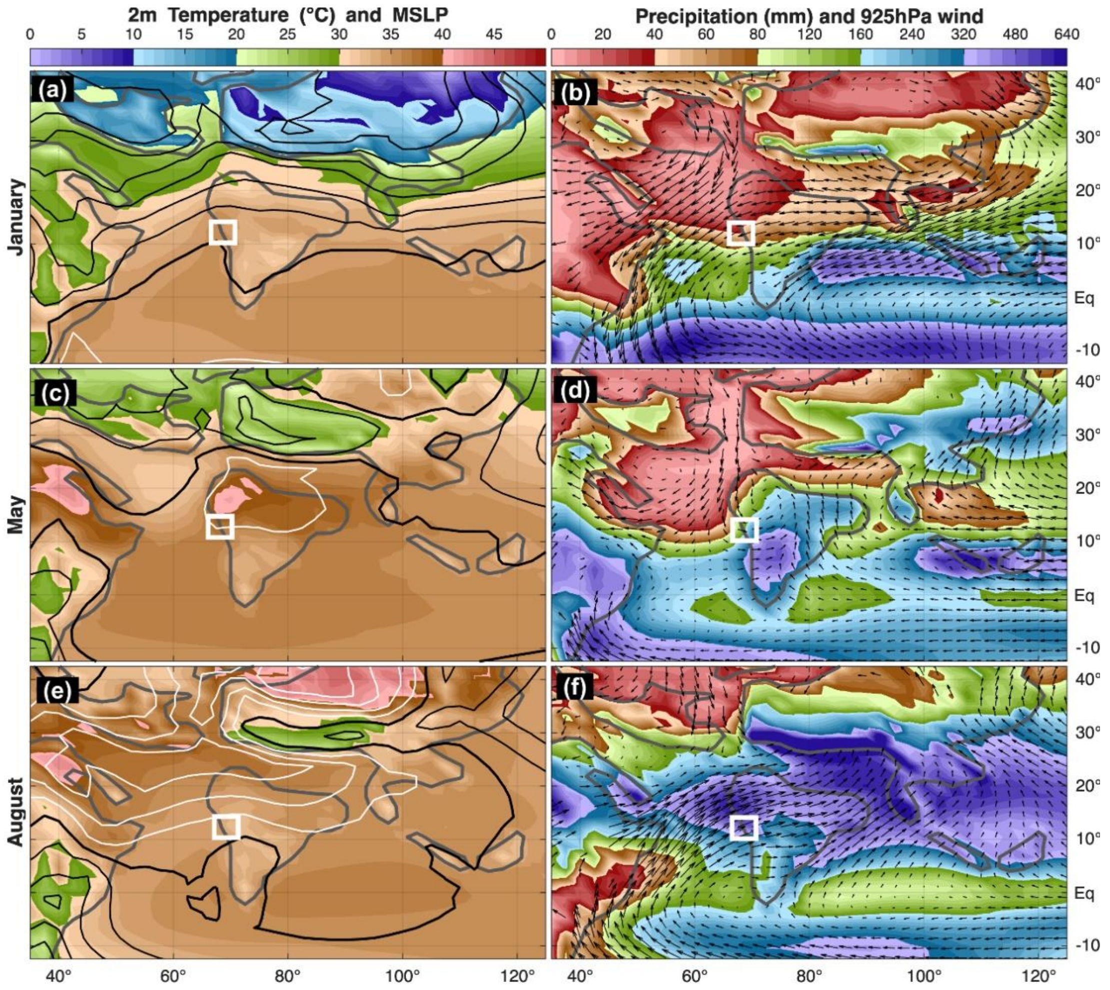

Figure 9. CESM outputs for the south Asian region at ~38 Ma under 2×PIC conditions in the months of January (post-monsoon rainfall month), May (peak summer) and August (monsoon): Left panels (a,c,e) show surface atmospheric air temperature at 2 m (shading) and mean sea level pressure (MSLP at 2.5 hPa intervals, white if <1000 hPa, thick black line at 1000 and 1020 hPa); Right panels (b,d,f) indicate precipitation (shading) and wind speed (length of arrows) and direction at 925 hPa. Study site is marked by white-boundary rectangle.

Figure 10: why are the y-axis gridlines not aligned in a,b,c? Are these not the same absolute values as this is confusing. Also, what do the red and blue lines in a,b,c mean, are they the modern SST and SAT as these are not the same colours as in the legend. And how did the Bartonian SST get calculated, is that from the CESM model simulation? The d,e,f panels are unclear with the stretched y-axis, please reconsider how to make this clearer. Consider adding the name of the region above the panels so the reader has a quick overview? The SAT are also distracting, not discussed, and should not be included.

Response: We thank you for pointing this out. We have revised Figure 10 to improve the consistency and clarity of the figure. In the original version, the plots were generated in Python without specifying common temperature limits, resulting in different y-axis ranges and automatically generated gridlines for panels (a-c). We have now standardised the y-axis scale across these panels.

The SAT data have been removed, as they were not discussed in the manuscript. In the original figure, the red lines represented SAT, whereas the blue lines represented SST. The revised figure has been updated accordingly to avoid confusion.

The Bartonian SST values shown in the revised figure are based on our clumped isotope temperature estimates (based on 9-11 replicates). We have also revised panels (d–f) to improve the presentation and readability of the y-axis. In addition, the names of the respective regions have been added above the panels to provide a clearer overview for the reader.

Please find Figure 10 in response to your **Line 380** related comment.

General language comments

Throughout the manuscript you change from early Bartonian vs late Bartonian or MECO vs post-MECO – be consistent.

Response: In the revised manuscript, we are consistent with mentioning ‘the early Bartonian’ and ‘the late Bartonian’.

Also include a definite article when describing a time period; “the” or “a” “early/late Bartonian”.

Response: We have added definite articles for defining a time period in the revised manuscript.

You mostly use palaeo- so I assume you are using British spelling but throughout have used paleo- in Lines 13, 57, 81, 240, 362, 369, 403, 444, 448, 531, 533, 534.

Response: We have corrected the spelling throughout the manuscript following the suggestion and now consistently use “palaeo”.

We have included all the new references in the revised manuscript following the in-text citations.